The Canadian Mineralogist
Vol. 49, pp. 835-847 (2011)
DOI : 10.3749/canmin.49.3.835

SANJUANITE: *AB INITIO* CRYSTAL-STRUCTURE SOLUTION FROM LABORATORY POWDER-DIFFRACTION DATA, COMPLEMENTED BY FTIR SPECTROSCOPY AND DT–TG ANALYSES

Fernando COLOMBO[§]

CONICET–CICTERRA, Cátedra de Geología General, Facultad de Ciencias Exactas, Físicas y Naturales,
Universidad Nacional de Córdoba, Vélez Sarsfield 1611, (X5016GCA) Córdoba, Argentina

Jordi RIUS

Institut de Ciència de Materials de Barcelona (CSIC), E–08193 Bellaterra, Catalonia, Spain

Elisa V. PANNUNZIO-MINER

INFIQC (CONICET), Departamento de Físico Química, Facultad de Ciencias Químicas, Universidad Nacional de Córdoba,
Ciudad Universitaria, (5000) Córdoba, Argentina

José C. PEDREGOSA and Gerardo E. CAMÍ

Área de Química General e Inorgánica, Departamento de Química, Facultad de Química, Bioquímica y Farmacia,
Universidad Nacional de San Luis, Chacabuco y Pedernera, (5700) San Luis, Argentina

Raúl E. CARBONIO

INFIQC (CONICET), Departamento de Físico Química, Facultad de Ciencias Químicas, Universidad Nacional de Córdoba,
Ciudad Universitaria, (5000) Córdoba, Argentina

Abstract

Sanjuanite, $Al_2(PO_4)(SO_4)(OH)\bullet 9H_2O$, is a microcrystalline fibrous mineral found in Pennsylvanian slates belonging to the Los Jejenes Formation at the Pocito Department, San Juan Province, Argentina. Sanjuanite is monoclinic, space group $P2_1/n$, with unit-cell dimensions a 13.9163(5), b 17.2422(5), c 6.1125(3) Å, β 98.255(4)°, V 1450.7(5) Å^3 and $Z = 4$. Its crystal structure has been solved and refined from laboratory powder-diffraction data (Bragg–Brentano geometry, Cu$K\alpha_{1,2}$ radiation, scintillation detector). Integrated intensities extending to a resolution of 1.15 Å were introduced in XLENS and processed with the S–FFT algorithm. Except for one O atom, the other atoms appeared in the Fourier map of the best direct-methods solution. Subsequent restrained Rietveld refinement converged to a χ^2 value of 2.47. The structure of sanjuanite is composed of infinite aluminophosphate chains running parallel to **c** and located at (x, y) = (0,0) and (½,½). Isolated $(SO_4)^{2-}$ groups and H_2O molecules connect the groups of chains. Hydrogen bonding plays a key role in the stabilization of the structure. The group formed by pairs of double chains of alternating (PO_4) and (AlO_6) present in sanjuanite bears no close resemblance to any known mineral structure. The FTIR spectrum and DTA–TGA curves of sanjuanite are provided. Chemically related species include kribergite and hotsonite, whose structures remain unknown. The formation of sanjuanite is probably related to the oxidation of sulfides (mostly pyrite and marcasite) under arid conditions, which produces sulfuric acid that releases Al from silicates in pelitic rocks. The source of P remains unknown.

Keywords: sanjuanite, aluminum phosphate–sulfate, crystal structure, chains of tetrahedra and octahedra, hydrogen bonding, Argentina.

[§] *E-mail address*: fcolombo@gtwing.efn.uncor.edu

SOMMAIRE

La sanjuanite, $Al_2(PO_4)(SO_4)(OH)•9H_2O$, minéral microcristallin fibreux, a été découvert dans les ardoises d'âge pennsylvanien faisant partie de la Formation Los Jejenes, département de Pocito, province de San Juan, en Argentine. La sanjuanite est monoclinique, groupe spatial $P2_1/n$, avec les paramètres réticulaires a 13.9163(5), b 17.2422(5), c 6.1125(3) Å, β 98.255(4)°, V 1450.7(5) Å^3 et Z = 4. Nous en avons résolu la structure et nous l'avons affiné avec des données prélevées en laboratoire par diffraction X, méthode des poudres (géométrie de Bragg–Brentano, rayonnement Cu$K\alpha_{1,2}$, détecteur par scintillation). Les intensités intégrées allant jusqu'à une résolution de 1.15 Å ont été introduites dans le logiciel XLENS et traitées avec l'algorithme S–FFT. Sauf pour un atome d'oxygène, les autres atomes étaient évidents dans la projection de Fourier de la meilleure solution obtenue par méthodes directes. Par la suite, un affinement de Rietveld avec contraintes a convergé à une valeur de χ^2 égale à 2.47. La structure de la sanjuanite est faite de chaînes aluminophosphatées infinies parallèles à **c** et situées à (x, y) = (0,0) et (½,½). Des groupes $(SO_4)^{2-}$ isolés et des molécules de H_2O servent à connecter les groupes de chaînes. Des liaisons hydrogènes jouent un rôle essentiel dans la stabilisation de la structure. Le groupe formé de paires de chaînes doubles dans la sanjuanite, ayant un alternance de (PO_4) et (AlO_6), semble unique parmi les structures connues de minéraux. Nous présentons le spectre FTIR et les courbes DTA–TGA de la sanjuanite. La kribergite et la hotsonite, dont les structures demeurent méconnues, ont certains points de ressemblance compositionnelle. La formation de la sanjuanite serait liée à l'oxydation de sulfures (surtout pyrite et marcasite) en conditions arides, ce qui a produit l'acide sulfurique qui a mobilisé l'aluminium des silicates des roches pélitiques. La source du P demeure méconnue.

(Traduit ar la Rédaction)

Mots-clés: sanjuanite, phosphate–sulfate d'aluminium, structure cristalline, chaînes de tétraèdres et d'octaèdres, liaisons hydrogène, Argentine.

INTRODUCTION

Sanjuanite, ideally $Al_2(PO_4)(SO_4)(OH)•9H_2O$, is one of the three known phosphate–sulfates containing Al as the only cation, the other two being hotsonite $Al_5(PO_4)(SO_4)(OH)_{10}•8H_2O$ (Beukes *et al.* 1984, Ivanov *et al.* 1990) and kribergite $Al_5(PO_4)_3(SO_4)(OH)_4•4H_2O$ (du Rietz 1945, Abeledo *et al.* 1968). The three minerals occur as polycrystalline aggregates composed of micrometric crystals. Therefore, structural information about them is rather limited, as they are not amenable to single-crystal studies, and other methods of indirect structural characterization have barely been applied to them.

Technological advances in X-ray generators and detectors, coupled with the availability of very intense monochromatic X-ray sources at synchrotron facilities, have dramatically decreased the minimum size of crystals needed for single-crystal studies. Now, complete atomic arrangements can be described using data measured in samples as small as 8 × 14 × 16 μm (Cahill *et al.* 2001, Chakhmouradian *et al.* 2008). However, several minerals occur as crystals even smaller than that, and so most of their structures remain unknown. Unless there is an isostructural compound that can be used as a starting point for a Rietveld refinement (Rietveld 1969), or an analogous material can be synthesized in larger crystals, the solution of their crystal structures using powder X-ray diffraction (PXRD) data is the only remaining approach. This is a very challenging task, mainly because of the collapse of three-dimensional data in one-dimensional space, with a concomitant loss of information. This becomes more complicated in low-symmetry structures, where peak overlap is very important at even moderate values of 2θ (>20°). Cheetham (1995) reviewed some of the difficulties inherent in structure solution using PXRD. In spite of these, some complex structures have been described [*e.g.,* tinticite: Rius *et al.* (2000), priceite: Wallwork *et al.* (2002), kingite: Wallwork *et al.* (2003), gormanite–souzalite series: Le Bail *et al.* (2003), parascorodite: Perchiazzi *et al.* (2004), aerinite: Rius *et al.* (2004), anthoinite: Grey *et al.* (2010)].

In this contribution, we describe the general structural features of sanjuanite, obtained using conventional powder X-ray diffraction data supplemented by Fourier-transformed infrared spectroscopy, differential thermal and thermogravimetric analysis.

PREVIOUS INFORMATION

Sanjuanite was discovered by Abeledo *et al.* (1968) in the eastern slope of the Sierra Chica del Zona, San Juan Province, northwestern Argentina. The precise coordinates of the type locality remain unknown, as those authors mentioned only that the occurrence is located "at about 45 km SSW from San Juan city and 12 km to the NNW from the mouth of the La Flecha canyon […], eastern slope of Sierra Chica del Zonda" (page 1). The mineral occurs in fossiliferous slates of Carboniferous age as conformable veinlets up to 5 cm thick, bounded by thin layers of gypsum. Other minerals present in fissures and mineralized diaclases in the same area, but not in contact with sanjuanite, are unspecified hydrated iron oxides, natrojarosite and alunite (Abeledo *et al.* 1968). The identity of this last species is rather uncertain, as Gordillo (one of the authors of the original description) reported results of an analysis of *natro*alunite from the same place, but alunite is not mentioned (Angelelli *et al.* 1983, p. 271–272). The chemical formula calculated from the analytical data (H_2O not considered, based on 11 O) is $(Na_{0.88}K_{0.04}Ca_{0.04})_{\Sigma 0.96}(Al_{2.93}Fe^{3+}{}_{0.06})_{\Sigma 2.99}(S_{2.01}O_8)$. The formula of natrojarosite (H_2O not considered, based on 11 O) is $(Na_{0.86}K_{0.14})_{\Sigma 1.00}(Fe^{3+}{}_{2.77}Al_{0.26}Ti_{0.01})_{\Sigma 3.05}(S_{1.93}P_{0.03})O_8$, according to the data given by the same authors.

Sanjuanite occurs as white compact masses consisting of micrometric acicular crystals, with a silky to a dull luster. The fine-grained nature of the material prevented the complete determination of some standard mineralogical data, like optical properties. Abeledo *et al.* (1968) published a table with X-ray-diffraction data, but they did not propose a unit cell or symmetry, other than mentioning that sanjuanite is either monoclinic or triclinic based on the clearly oblique extinction (up to 30°) of the fibers. Attempts to obtain crystallographic information using electron diffraction were hampered by the fact that sanjuanite dehydrates readily under a high vacuum, giving an amorphous material.

De Bruiyn *et al.* (1989) found that the X-ray diffraction data given in the original description could be indexed on the basis of a triclinic unit-cell, with *a* 11.314, *b* 9.018, *c* 7.376 Å, α 93.07, β 95.775, γ 105.32°. It should be stressed that this conclusion was reached only using published information, and no new measurements were performed. Although most peaks were appropriately accounted for, two reflections located at 6.92 Å ($I/I_0 = 8\%$) and at 4.27 Å ($I/I_0 = 30\%$) remained unexplained and were attributed to an unknown contaminant.

The only other known occurrence of sanjuanite is located in Yakutia, Russia (Lazebnik *et al.* 1998). The same peaks in the powder X-ray-diffraction pattern attributed to the contaminant are also present in the Russian sanjuanite, with similar relative intensities, suggesting that they indeed belong to sanjuanite and are not due to an admixed compound.

THE SANJUANITE LOCALITY

The only formation that matches the information given by Abeledo *et al.* (1968) is the Jejenes Formation (Amos 1954) of Upper Carboniferous (Pennsylvanian: Westphalian–Stephanian) age, which rests on Cambrian–Ordovician limestones, separated by an angular unconformity. This formation was deposited in a highly confined fjord and is composed of diamictites overlain by a mudstone-dominated succession with intercalations of sandstone and conglomerate. The upper part of the formation consists of more than 300 m of sandy turbidites. The Jejenes Formation has been studied as an example of catastrophic sedimentation (Kneller *et al.* 2004, Dykstra *et al.* 2006). Even though fossil plants are found throughout the formation, the upper part of the sequence is especially remarkable for the abundant paleoflora belonging to the NBG biozone that characterizes the Upper Carboniferous of Argentina (Pujana 2005).

There is no specific information about the origin of sanjuanite, other than the statement of Abeledo *et al.* (1968) that it is possibly related to ascending acidic hydrothermal solutions. In San Juan Province, there are several concentrations of sulfates of Al, Mg, Zn and Fe (copiapite, botryogen, coquimbite, slavíkite, butlerite, parabutlerite, voltaite, melanterite, goslarite, amarantite, hexahydrite, halotrichite, pickeringite, epsomite, alunogen, fibroferrite, and szomolnokite, among others: Angelelli *et al.* 1983), most of them located in the Calingasta Department, northwest of the sanjuanite location. Mining for sulfates using open-pit methods reached its maximum during the 1970s, where over 54,000 tonnes were mined annually (Cardinali 1999). These sulfate concentrations originate by weathering of Fe sulfides or are part of an intrusion-related hydrothermal alteration halo.

In the first case, the origin of sulfur is related to the weathering under arid conditions of syngenetic sulfides in the pelites (the most abundant being pyrite and marcasite). The percolating acidic solutions decompose Al silicates, especially clays, releasing Al, which precipitates as Al sulfates in cracks deeper in the profile (Cardinali 1985). The hydrothermal alteration related to a cooling magmatic chamber is of acid-sulfate type and is restricted to porphyritic andesites. This is the origin of sulfate accumulations at the Cura Valley (Cardinali 1999).

Unless the original occurrence is located, any hypothesis will remain speculative; however, we favor the possibility of sanjuanite precipitation due to percolating solutions, as no evidence of magmatic activity is noted in the area. The origin of the phosphorus remains unknown. This seems to be the case also for hotsonite, $Al_5(PO_4)(SO_4)(OH)_{10}•8H_2O$ (Schoch *et al.* 1985).

SAMPLE DESCRIPTION

The sanjuanite sample studied belongs to the collection of the Museo de Mineralogía y Geología "Dr. A. Stelzner" of the Universidad Nacional de Córdoba, Argentina (catalog number 1461). It is a 8.5 × 4 × 3 cm fragment of chalk-white color, composed of a mass of extremely thin fibers of sanjuanite in radial or parallel aggregates, with some incrustations of scaly colorless gypsum and unidentified clay minerals (Fig. 1). No matrix is present. It was donated by Mr. E. Aparicio, who also furnished Abeledo *et al.* (1968) with the samples used in the original description.

The chemical composition reported by those authors (wt%, mean and standard deviation of three analyses performed on two different samples) is 16.27(0.15) P_2O_5, 18.82(0.18) SO_3, 23.93(0.40) Al_2O_3, 1.53(0.17) Fe_2O_3 and 40.05(0.19) H_2O, total 100.60(0.18), with little difference between the samples. The empirical formula, calculated on 18 O, is $(\mathrm{Al}_{1.99}\mathrm{Fe}^{3+}_{0.08})_{\Sigma 2.07}(\mathrm{P}_{0.97}\mathrm{O}_4)(\mathrm{SO}_4)(\mathrm{OH})\bullet 8.95\mathrm{H}_2\mathrm{O}$. In addition to the main constituents, EDS spectra of the sample studied by us show trace amounts of Si and Ca.

EXPERIMENTAL METHODS

Images and standardless analyses were obtained on a carbon-coated sample with a Philips SEM 515 scanning electron microscope equipped with an energy-dispersive analyzer. The powder X-ray diffraction pattern was collected on a Philips PW1710 diffractometer with Bragg–Brentano geometry, Cu$K\alpha_{1,2}$ radiation and a graphite secondary monochromator (measured 2θ interval: 3° to 100°, step size 0.015° 2θ, counting time: 10 s per step). The pattern contained no useful information beyond 2θ = 100°. Information about the procedures leading to the structure solution is given in the corresponding section.

The Fourier-transformed infrared (FTIR) spectrum was recorded between 4000 and 250 cm^{-1} with a Nicolet Protégé 460 spectrometer with Omnic Software, using a standard pressed-disk technique, after embedding 1 mg of mechanically ground sanjuanite in 200 mg of dry KBr and compacting it using a pressure of 500 kg cm^{-2}. Spectral resolution is better than 2.0 cm^{-1} between 4000 and 2000 cm^{-1}, and better than 1.0 cm^{-1} in the remaining range.

Thermogravimetric (TG) and differential thermal analysis (DTA) curves were obtained with a Shimadzu TGA–50H/DTA–50 thermal analyzer apparatus at a heating rate of 10°C min^{-1} from room temperature to 1,000°C, using flowing air at 50 mL min^{-1}.

AB INITIO CRYSTAL-STRUCTURE SOLUTION AND REFINEMENT USING LABORATORY POWDER X-RAY DIFFRACTION

The powder pattern of sanjuanite was successfully indexed with TREOR90 (Werner 1984). The unit cell is monoclinic, a 13.9163(5), b 17.2422(5), c 6.1125(3) Å, β 98.255(4)°, V 1450.7(5) Å^3 and $Z = 4$. Systematic absences suggest that sanjuanite crystallizes in space group $P2_1/n$ (#14). The indexed powder-diffraction data have been incorporated to the Powder Diffraction Files as card #07227 (note that the space group of that card is $P2_1/a$, an unconventional choice); it closely matches that reported by Lazebnik *et al*. (1998). A previous attempt to fit the PXRD pattern using the unit cell of de Bruiyn *et al*. (1989) gave unsatisfactory results. However, all peaks (including those at 6.92 and 4.27 Å mentioned above) are adequately explained by the unit cell we propose.

A very small non-indexed peak corresponding to the strongest line of gypsum appears at a d value of 7.54 Å. This is not surprising, as mm-sized grains of gypsum were observed in the hand sample from which the sanjuanite powder was extracted. Owing to its irrelevance, the presence of this very small gypsum impurity was not considered in the powder-diffraction study. This peak is not present in the sample studied by Lazebnik *et al*. (1998).

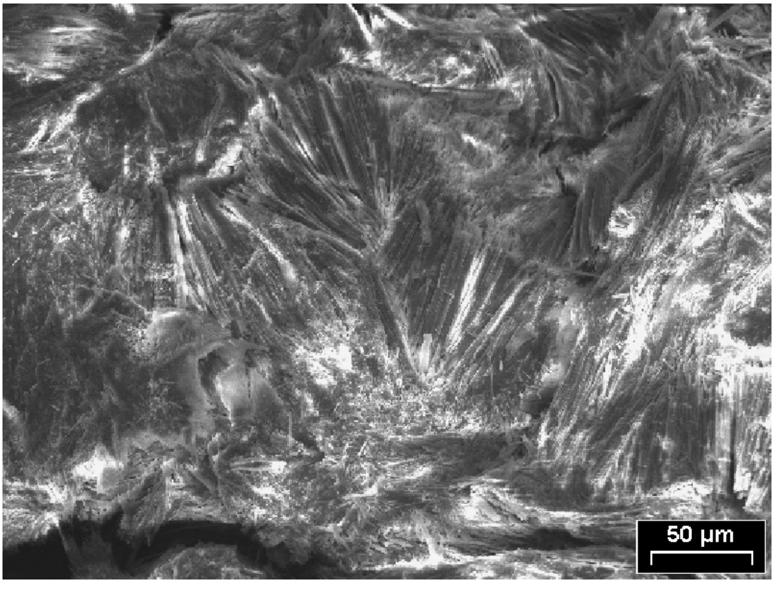

FIG. 1. SEM image of sanjuanite, showing the fibrous nature of the aggregates.

Integrated intensities to 1 Å resolution were extracted with the whole-pattern matching (wpm) algorithm described in Rius *et al.* (1996) and implemented in DAJUST1 (Rius 2009b). The background was estimated according to Brückner (2000). The breadths of the diffraction peaks, refined with FWHM ranging between 0.13 and 0.09° 2θ, are considerable. The extracted intensities with $d > 1.15$ Å were further processed with an improved version of the S–FFT direct methods algorithm (Rius 2011) implemented in XLENS (Rius 1993). With the exception of O8 (the O atom that is closest to Al2), all other non-H atoms clearly showed up in the Fourier synthesis computed with the refined phases from the best solution. Once the crystal-structure model was completed, it was refined with the Rietveld program RIBOLS18 (Rius 2009a). Owing to the complexity of the structure (low symmetry and large unit-cell, leading to a high degree of overlap of reflections) and the fact that the diffractogram was measured using conventional X-radiation (with the typical resolution expected for this equipment), the introduction of restraints was necessary to ensure meaningful distances and to reduce the risk of false minima (Bärlocher 1995). Introduced restraints were 1.485(5) Å for S–O, 1.540(15) Å for P–O, 1.910(5) Å for Al1–O, and 1.910 Å for Al2–O (values of e.s.d. 0.02 except 0.04 Å for O8). The large number of H atoms in the structure caused the refined atomic displacement parameters B to be slightly high (4.1 Å^2). The fibrous character of sanjuanite causes preferred orientation if it is mounted on a flat sample holder. The preferred orientation is given by the reciprocal space vector [$\bar{2}$03], which runs parallel to the aluminophosphate chains along the **c** axis. General information about the refinement and residual indices appears in Table 1. Final coordinates expressed according to the standard and reduced cell, *a* 13.9163(5), *b* 17.2422(5), *c* 6.1125(3) Å, β 98.255(4)°, $P2_1/n$, are listed in Table 2; the Rietveld plot showing the good agreement between observed and calculated patterns is reproduced in Figure 2.

Sanjuanite has a rather low density; the calculated value with $Z = 4$ is 1.95 g cm^{-1}, in very good agreement with the measured value of 1.94 g cm^{-1} given by Abeledo *et al.* (1968).

DESCRIPTION OF THE STRUCTURE

Sanjuanite is a hydrated sulfate with aluminophosphate units running parallel to the **c** direction and placed at (x, y) = (0,0) and (1/2,1/2) (Fig. 3). As explained below, the O10, O11, O12, O13, O14 and O15 atoms shown in Figure 4 correspond to H_2O molecules coordinating the Al atoms, whereas atom O9 denotes the hydroxyl group linked to two Al atoms. The O atoms O16, O17, O18 are free H_2O molecules.

The aluminophosphate unit (APU)

As illustrated in Figure 4, this unit can be best described as double chains of alternating Al and P atoms repeating along the **c** direction, giving rise in this way to the bond sequence (Al2–O6–P1–O8–Al2'–...); consequently, the Al2–O octahedra share two corners with the neighboring phosphate groups. The two chains are related by a center of symmetry and joined together by two symmetry-related Al1–O octahedra. This addi-

TABLE 1. SUMMARY OF RELEVANT INFORMATION FOR THE RIETVELD REFINEMENT OF SANJUANITE

Unit-cell parameters	
a, *b*, *c*	13.9163(5), 17.2422(5), 6.1125(3) Å
β	98.255(4)°
Unit-cell volume, *Z*	1450.7(5) Å^3, 4
Space group	$P2_1/n$ (#14)
Radiation, wavelength	Cu$K\alpha_{1,2}$, 1.54059, 1.54443 Å
2θ range	5.995 -100.000°
Number of data points	6268
Peak range in FWHM	20
Number of contributing reflections	1440
Number of profile parameters	10
Number of structural parameters	68
Number of structural restraints	27
Profile function	pseudo-Voigt
Peak breadth	0.13° at 2θ =20°, 0.09° at 2θ = 85°
March–Dollase coefficient	1.20(2)
Preferred orientation direction	[$\bar{2}$ 0 3]
Zero shift	–0.0661(5)°
Background estimation	see Experimental
R_{wp}, χ^2	0.097*, 2.47
Weighting scheme	$1/y_o$

* *R* values as defined in Langford & Louër (1996).

TABLE 2. FINAL REFINED COORDINATES OF ATOMS IN SANJUANITE

Atom	*x/a*	*y/b*	*z/c*	Occupancy
S1	0.1264(5)	0.3459(4)	0.4154(16)	1
P1	0.1212(7)	0.0463(6)	0.6855(26)	1
Al1	-0.1099(7)	0.1155(6)	0.5944(22)	1
Al2	0.1809(8)	0.0688(7)	1.2090(25)	1
O1	0.0730(10)	0.3868(8)	0.5733(23)	1
O2	0.1157(10)	0.3795(9)	0.1902(22)	1
O3	0.2312(6)	0.3494(9)	0.5123(30)	1
O4	0.0968(11)	0.2635(5)	0.3956(32)	1
O5	0.1090(13)	-0.0425(8)	0.6397(28)	1
O6	0.1781(13)	0.0826(10)	0.5138(28)	1
O7	0.0276(8)	0.1010(11)	0.6646(40)	1
O8	0.1748(13)	0.0547(12)	0.9249(32)	1
O9	-0.1507(13)	0.0399(8)	0.7903(32)	1
O10	-0.0790(13)	0.1981(10)	0.4080(31)	1
O11	-0.2432(7)	0.1385(11)	0.4860(31)	1
O12	-0.1104(12)	0.1930(10)	0.8185(27)	1
O13	0.3208(9)	0.0524(11)	1.2296(40)	1
O14	0.0469(11)	0.0993(10)	1.1403(40)	1
O15	0.2149(13)	0.1798(9)	1.1860(45)	1
O16	-0.0173(11)	0.3300(9)	0.8685(37)	1.25*
O17	-0.1028(12)	0.4512(9)	0.2361(38)	1.25*
O18	0.3053(11)	0.1940(11)	0.8001(39)	1.25*

* to take into account the scattering power of the H atoms in the H_2O molecule. Values of e.s.d. are given in parentheses. One overall *B* value has been used for all atoms, 4.1(1) Å^2, except for O16, O17, O18 [8.5(2) Å^2]. All atoms are in general positions.

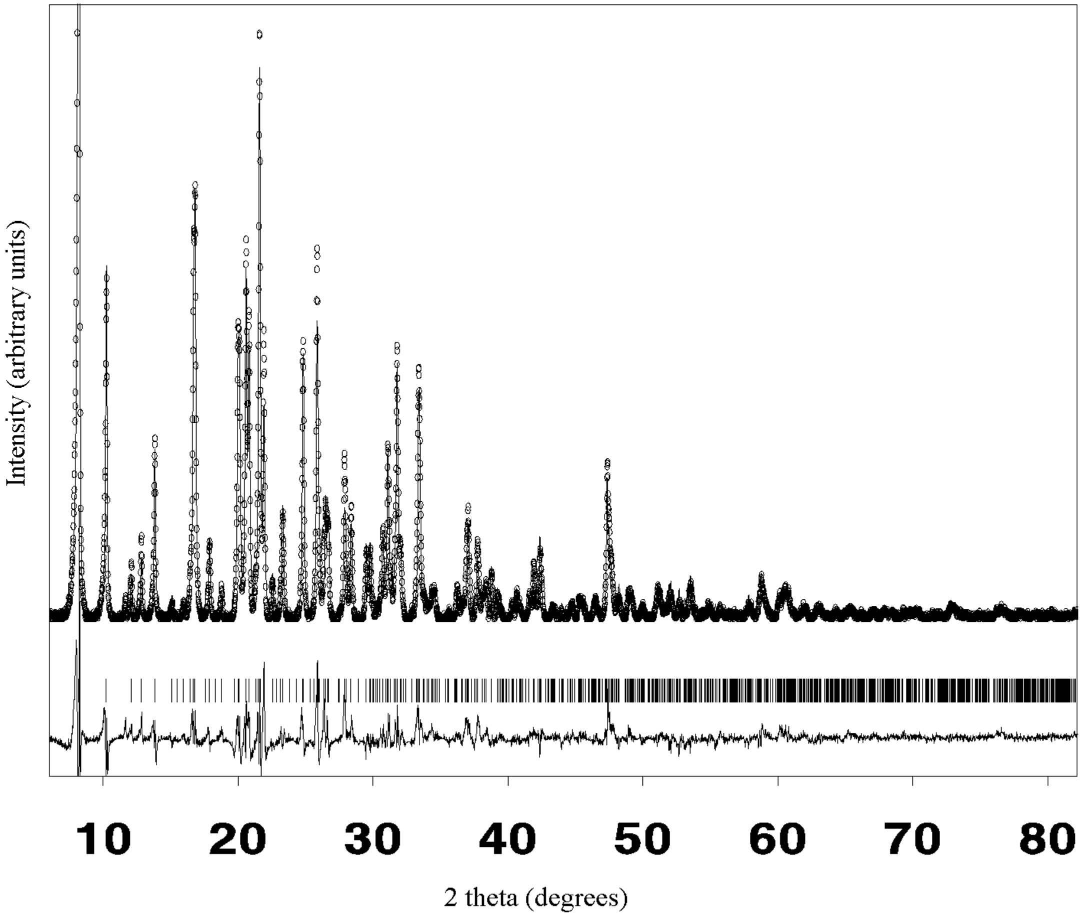

FIG. 2. Final Rietveld plots of sanjuanite. The calculated pattern is represented by a solid line and the observed data by circles. The lower trace is the difference between observed and calculated profiles. The vertical markers show positions calculated for Bragg reflections.

tional octahedron shares three corners with the double chain polyhedra, *i.e.*, the bridging O atoms (O9, O5 and O7'). This arrangement produces a three-membered ring defined by the P1–O6–Al2–O9–Al1–O5–(P1) sequence of bonds. Alternatively, the aluminophosphate unit could be seen as a chain formed by corner-sharing pairs of AlO_6 octahedra (each pair formed by Al1 and Al2) connected by (PO_4) tetrahedra.

The ideal Al–O bond strength for octahedrally coordinated Al is 0.5 valence units (*vu*). Similarly, the ideal P–O bond strength for tetrahedrally coordinated P is 1.25 *vu*. According to the results of the refinement, O9 displays no significant interaction with atoms other than Al1 and Al2, so that its formal charge must be close to 1 *vu* (0.5 from Al1 + 0.5 from Al2). Hence, O9 must correspond to a hydroxyl group. The other two bridging O atoms of the Al1–O octahedron (O5 and O7) form probable H-bonds with O14. If the P–O and H bond strengths are assumed to be 1.25 and 0.25 *vu*, respectively, the ideal formal charge of 2 *vu* (= 1.25 + 0.5 + 0.25) for O5 and O7 is reached. Finally, the three terminal O atoms (O12, O13, O14 and O15) must be H_2O molecules. The excess charge (≈ 0.5 *vu* on average) at each terminal O atom (*i.e.*, O12, O13, O14 and O15) requires these atoms to correspond to H_2O molecules, so that it can be transferred *via* H-bonds to the sulfate groups either directly or through the free H_2O molecules (O16, O17, O18). The details of the probable H bonds involving O12, O13 and 14 are given in Table 3.

Besides the O9 hydroxyl, the Al2–O octahedron has two more bridging O atoms, O8 and O6. Because O8 has no neighbors at H bond distance, the strength of the

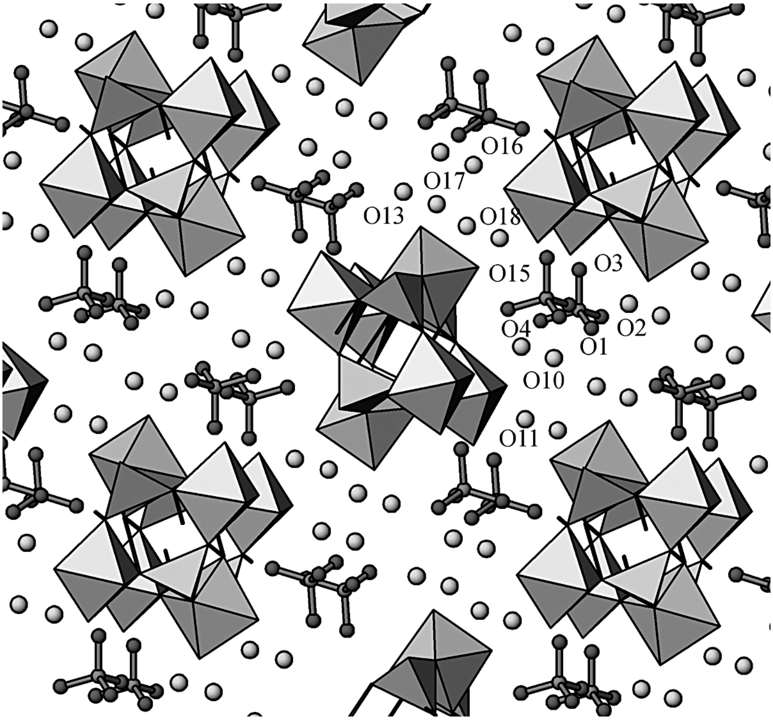

FIG. 3. Perspective view of sanjuanite along **c** (**a** down and **b** across the page). The aluminophosphate units can be clearly seen centered at (x,y)= (0,0) and (1/2,1/2). The sulfur atoms with their O atoms (O1, O2, O3, O4) and the free H_2O molecules (O16, O17, O18) are placed in between.

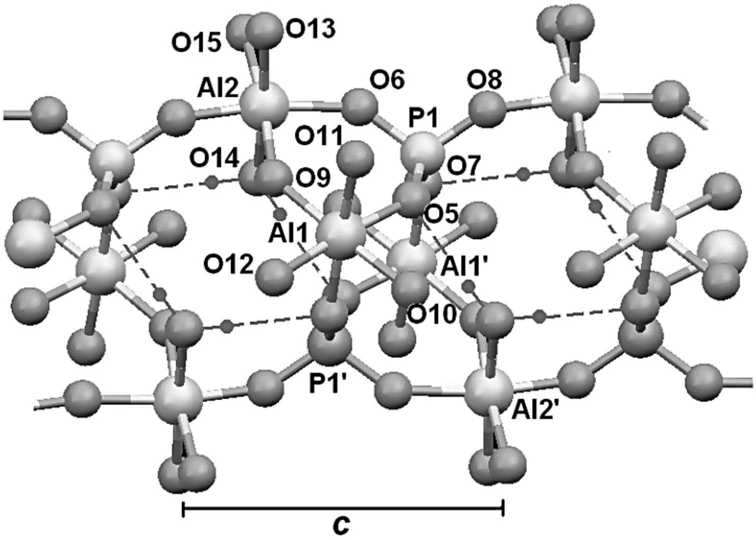

FIG. 4. Portion of the aluminophosphate unit with atom numbering (atoms marked with ' are related by a center of symmetry). The chain of alternating Al2–O octahedra and P1–O tetrahedra is linked to the symmetry-related one through the two symmetry-related Al1–O octahedra. Considered important to ensure the stability of the unit are the probable O14–H…O5' and O14–H…O7' H bonds, which are represented as dashed lines.

Al–O bond must be close to 0.75 *vu*, *i.e.*, 1.25 + 0.75 = 2 *vu*. The shorter refined Al2–O8 bond length (*i.e.*, 1.75 instead of 1.91 Å) supports this point. In the case of O6, owing to the proximity of the O18 H_2O molecule, it probably acts as an acceptor of an H bond. If an H bond strength of 0.25 *vu* is assumed, the bond-valence sum for O6 is exactly 2 *vu* (= 1.25 + 0.50 + 0.25). By adding up the contributions of the bridging O atoms, the partial bond-valence sum for Al2 is 1.75 *vu* (= 0.75 + 0.5 + 0.5). As Al is trivalent, each one of the three terminal O atoms (O13, O14 and O15) thus has on average an excess charge of 0.42 *vu*, which must be transferred to the sulfate groups either directly or through the H_2O molecules (O16, O17, O18) *via* the formation of H bonds. Table 3 summarizes the probable H bonds.

In addition to the six symmetrically independent coordinated H_2O molecules, the unit cell also contains three more H_2O molecules not directly bound to Al, which are indispensable for the H bond network. The O17 (O18) H_2O molecule is located approximately halfway between consecutive O13 (O15) atoms along the **c** direction. In a certain sense, they play the role of O10, which is also placed between consecutive O12 atoms, and greatly facilitate the formation of the H bond network.

TABLE 3. APPROXIMATE BALANCE OF BOND VALENCES (*vu*) FOR SANJUANITE

Atom (*X*)	S1	P1	Al1	Al2	Σ_C v	Probable H bonds				O··*X*··O (°)
O1	**1.50** 1.48				**1.50**	**← O16** 2.7	**← O17** 3.0			
O2	**1.50** 1.48				**1.50**	**← O11** 2.5	**← O16** 2.6	**← O13** 3.1		
O3	**1.50** 1.50				**1.50**	**← O12** 2.7	**← O11** 2.8			
O4	**1.50** 1.48				**1.50**	**← O10** 2.7	**← O15** 2.7			
O5		**1.25** 1.56	**0.50** 1.91		**1.75**	**← O14** 2.9				
O6		**1.25** 1.54		**0.52** 1.88	**1.77**	**← O18** 3.0				
O7		**1.25** 1.60	**0.50** 1.92		**1.75**	**← O14** 2.9				
O8		**1.25** 1.55		**0.74** 1.74	**1.99**	**-**				
O9(H)			**0.50** 1.91	**0.46** 1.92	**0.96**	**-**				
O10(w)			**0.50** 1.91		**0.50**	**→ O18** 2.5	**→ O4** 2.7			104
O11(w)			**0.50** 1.92		**0.50**	**→ O2** 2.5	**→ O3** 2.9			121
O12(w)			**0.50** 1.91		**0.50**	**→ O3** 2.7	**→ O16** 2.7			126
O13(w)				**0.43** 1.95	**0.43**	**→ O2** 3.1	**→ O16** 3.1			114
O14(w)				**0.45** 1.93	**0.45**	**→ O5** 2.9	**→ O7** 2.9			120
O15(w)				**0.40** 1.98	**0.40**	**→ O4** 2.7	**→ O18** 2.8			137
O16(w)					**0.00**	**← O12** 2.7	**← O13** 3.1	**→ O1** 2.7	**→ O2** 2.6	108
O17(w)					**0.00**	**← O18** 2.9	**→ O1** 3.0			142
O18(w)					**0.00**	**← O10** 2.5	**← O15** 2.8	**→ O6** 3.0	**→ O17** 2.9	108
Σ_A v	6	5	3	3						

Owing to the expected regularity of their coordination polyhedra and to the large uncertainty in the cation–O distances (s.u.s ≈ 0.02 Å), ideal bond-valences v_i (upper value in bold) are assumed for S1, P1 and Al1; for Al2, they are estimated from the individual Al–O distances d_i (lower value in Å), with expression $v_i = K_{Al}\, d_i \exp(-p_{Al} d_i)$, where $p_{Al} = 3.13$ is taken from Rius & Plana (1982) and Allmann (1975), and $K_{Al} = 98.6$ is fitted to the individual coordination polyhedron to satisfy the charge of Al^{3+}. Owing to the low accuracy of the O…O distances (s.u.s ≈ 0.1 Å), only the donor (→) or acceptor (←) character of each probable H bond is given. In the last column, the value of the O…*X*…O angle (°) is listed (except for O16 and O18 in a tetrahedral environment, where it corresponds to the average of the six O…*X*…O angles).

FOURIER-TRANSFORM INFRARED SPECTROSCOPY

Figure 5 shows the FTIR spectrum of sanjuanite at room temperature in the region 4000–250 cm^{-1}. The proposed assignment of bands in this spectrum appears in Table 4. The vibrational behavior of sanjuanite is expected to be rather complex, taking into account that the structure consist of several different polyhedra. A digital version of the FTIR spectrum is available from the Depository of Unpublished Data on the MAC website [document Sanjuanite CM49_835].

TABLE 4. INFRARED VIBRATIONAL SPECTRUM OF SANJUANITE

Wavenumber (cm^{-1})	Tentative assignment
3575 (w)	$\nu(OH)^-$
3375 (s–w)	$\nu_3(H_2O)$ (coordinated)
3180 (s–w)	$\nu_3(H_2O)$ (between chains)
2495 (w)	overtone $(PO_4)^{3-}$
1650 (m)	bending H_2O (total)
1130 (sh)	$\nu_3(SO_4)^{2-}$
1075 (s)	$\nu_3(PO_4)^{3-}$
983 (w)	$\nu_1(SO_4)^{2-}$
830 (m)	antisymmetric stretching Al–O–P
709 (sh)	librational modes H_2O
650 (m)	librational modes H_2O
630 (m)	$\nu_4(SO_4)^{2-}$ [+ νs(Al–O–P)?]
588 (m)	$\nu_4(PO_4)^{3-}$ + librational (H_2O)
517 (sh)	AlO_6 stretching
460 (m)	$\nu_2(SO_4)^{2-}$
410 (sh), 386 (vw), 375 (vw), 360 (sh), 320 (m),300 (sh), 250 (w)	deformations (lattice modes + Al–O)

s–w (strong–wide), s (strong), vs (very strong), m (medium), w (weak), vw (very weak), sh: shoulder.

The internal vibrations can be described by means of the following building units: H_2O molecules and hydroxyl, sulfate, phosphate, Al–O–H, and Al–O–P groups.

H_2O and $(OH)^-$ modes

The presence of two kinds of crystallographically non-equivalent H_2O molecules in the lattice is established by their characteristic vibrational modes in the FTIR spectrum. In the O–H stretching region, the sharp band at 3575 cm^{-1} is assigned to hydroxyl mode ν(OH). Two broad bands centered at 3375 and 3180 cm^{-1} are assigned to the stretching mode $\nu_3(H_2O)$ of the two types of H_2O molecules in the lattice. The first is coordinated to the Al atoms, and the other forms the H bonds connecting the groups of chains found by structure analysis. According to the bond distance – frequency correlation given by the equation of Libowitzky (1999), these frequencies correspond to the O–H...O distances 2.782 and 2.706 Å, respectively. The band at 2495 cm^{-1} has a comparatively low wavenumber, which suggests strong H-bonding, and coincides with the shorter O–H...O distance that characterizes the hydrogen bond within the $(HPO_4)^{2-}$ group. However, the $(HPO_4)^{2-}$ ion also has some very characteristic bands between 950 and 1265 cm^{-1} (Moraes *et al.* 2006) that are not observed in the sanjuanite spectrum. It could be argued that these bands overlap with modes of the $(PO_4)^{3-}$ or $(SO_4)^{2-}$ ions; however, the absence of bands corresponding to $\nu_{as}(PO_4)$ at wavenumbers higher than

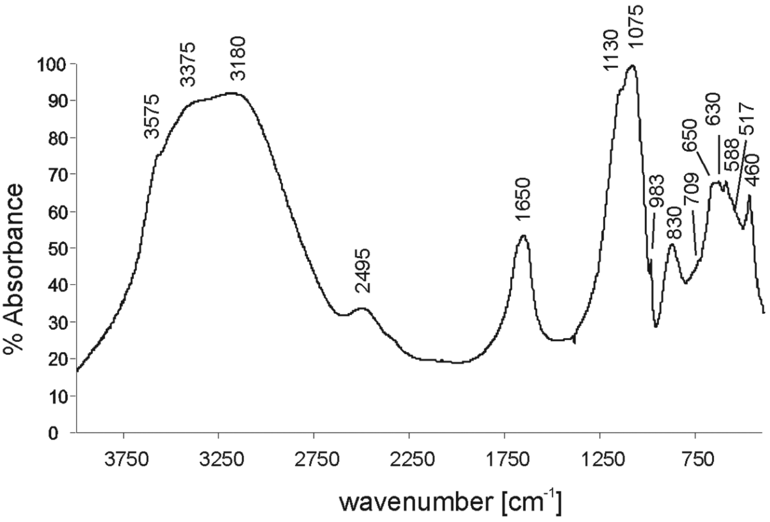

FIG. 5. FTIR spectrum of sanjuanite at room temperature in the region between 4000 and 250 cm^{-1}.

1150 cm^{-1} clearly indicate that $(HPO_4)^{2-}$ is not present in sanjuanite. Therefore, in concordance with Moraes *et al.* (2006), we have assigned the band at 2495 cm^{-1} to an overtone.

The H–O–H bending of H_2O occurs at 1650 cm^{-1}. The librational modes of H_2O, which usually exhibit a low intensity and overlap with other modes, are difficult to identify. Weak bands occur in the FTIR spectrum at approximately 709, 650 and 588 cm^{-1} and are associated to librational modes, mainly wagging and rocking, involving H_2O molecules in a crystalline environment (Assaoudi & Ennaciri 1997).

Stretching region of sulfate and phosphate groups

The simplicity of the recorded FTIR spectrum suggests a limited influence of correlation field effects (derived from vibrational coupling in the unit cells), precluding an analysis by site symmetry or factor group. On this basis, the XO_4 (X = P or S) units could be expected to behave as approximately isolated groups. The highly ionic character of the $(SO_4)^{-2}$ ion is responsible for this behavior, experimentally demonstrated by the presence of sharp bands without splitting, although activation of symmetric modes is observed. In the stretching region, we have assigned the 1130 and 983 cm^{-1} bands to the $\nu_3(F_2)(SO_4)^{2-}$ and $\nu_1(A_1)(SO_4)^{2-}$, respectively. These values are in agreement with those of other mineral sulfates (Myneni 2000, Márquez Zavalía & Pedregosa 1994).

The symmetry generated by the three-membered ring defined by the P1–O6–Al2–O9–Al1–O5–(P1) sequence of tetrahedra and octahedra sharing corners does not influence the splitting and activation of the P–O modes. Because of the rigidity of the ring containing these polyhedra, the infrared spectrum cannot be interpreted in terms of localized vibrations, the atoms of the ring being involved in several vibrational modes. However, the band in 1075 cm^{-1} is tentatively assigned to ν_{as}(P–O) in the chain.

The band at 830 cm^{-1} is assigned to the antisymmetric mode of the bridge Al–O–P vibrating as a whole in the chains of the crystal. Its appearance is conclusive evidence for the bent Al–O–P configuration (Baran *et al.* 1974, Castro Luna *et al.* 1994). It is also possible that the band at 630 cm^{-1} [assigned to $\nu_4(SO_4)^{2-}$] has some intensity attributable to the symmetric mode of the Al–O–P bridge.

The spectroscopic behavior of the $(SO_4)^{2-}$ group located between the chains and of the $(PO_4)^{3-}$ groups belonging to the P–O–Al chains is clearly different owing to the limited impact of correlation field effects on the sulfate anion. The lowering of the lattice symmetry activates the ν_1 and ν_2 modes of the sulfate anion (this phenomenon occurs in most of the ionic natural sulfates and phosphates). In contrast, $(PO_4)^{3-}$ has a different symmetry, such that no activation of the symmetric modes is observed. These results lend additional support to the crystallographic data obtained from X-ray diffraction.

Bending modes and other low-wavenumber bands

The medium- to low-wavenumber region on the FTIR spectrum is quite complex; $(PO_4)^{3-}$ and $(SO_4)^{2-}$ bending, and AlO_6 stretching vibrations contribute to the absorption in the 650–500 cm^{-1} region. On the basis of the intensity of the bands and the findings of Müller & Krebs (1967), we have made a tentative assignment. Bands at 630, 588 and 517 cm^{-1} are assigned to antisymmetric $\nu_4(F_2)$ of $(SO_4)^{2-}$, antisymmetric $\nu_4(F_2)$ of $(PO_4)^{3-}$ and AlO_6 stretching, respectively. The band at 460 cm^{-1} includes the symmetric $\nu_2(E)$ of $(SO_4)^{2-}$. In addition, the lower-energy bands are related to lattice modes.

THERMOGRAVIMETRIC AND THERMAL-DIFFERENTIAL ANALYSES

The DTA curve of sanjuanite (Fig. 6) shows a signal at 137°C corresponding to a dehydration process. The loss occurs as a sharp endothermic peak with a shoulder toward the low-temperature end, probably reflecting the sequential loss of H_2O from the two non-equivalent sites. The experimental loss in mass, 38.24%, corresponds to 9 H_2O molecules (theoretical value: 38.20 wt%). This dehydration temperature is lower than that observed by Abeledo *et al.* (1968) and Lazebnik *et al.* (1998), who recorded temperatures of *ca.* 190°C (note that Abeledo *et al.* 1968 gave a different figure in the text and their Fig. 4; the *ca.* 190°C value was obtained from their Fig. 3). However, it is known that the heating rate and grain size of the sample influence the temperature at which an effect is detected in DTA–TGA studies, so at least part of the difference could be attributed to this cause.

The next change can be seen at 847°C, corresponding to a sharp endothermic peak in the DTA curve, with an experimental loss in mass of 19.70%, attributed to the loss of hydroxyl and $(SO_4)^{2-}$ groups (the calculated value is 21.00 wt%).

An XRPD pattern of the residue after heating to 500°C shows broad peaks corresponding to a poorly crystalline mixture of two anhydrous aluminum phosphates (probably monoclinic and orthorhombic $AlPO_4$, PDF #511674 and #721161, respectively). The DTA–TGA curves and mass-balance considerations indicate that the remaining Al, S, O and H (± P) must be accommodated by one or more amorphous phases. The residue after heating to 1,000°C has a PXRD pattern very similar to the one described above.

RELATIONSHIP OF SANJUANITE WITH OTHER SPECIES

As mentioned in the introduction, sanjuanite shares strong chemical similarities with hotsonite

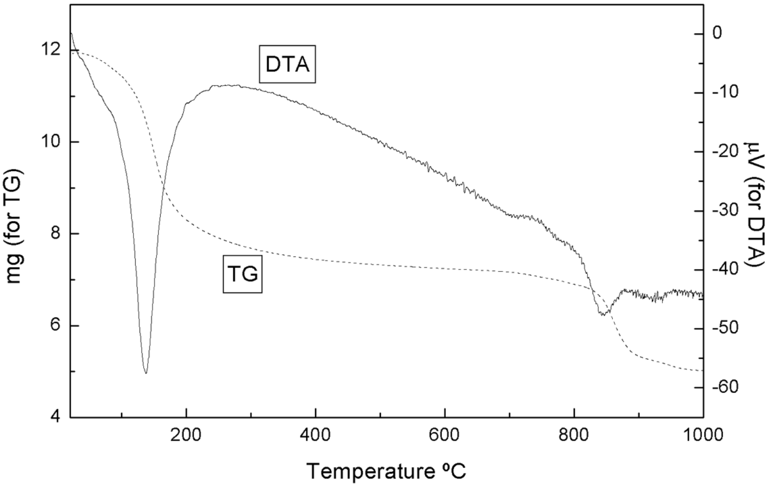

FIG. 6. DTA (solid line) and TG (dotted line) curves for sanjuanite.

and kribergite. Unfortunately, the crystal structures of these two minerals remain unknown, so no further comparison is possible. Mitryaevaite, $Al_5[(PO_4)_2(P,S)O_3(OH,O)]_2F_2(OH)_2(H_2O)_8 \bullet 6.48H_2O$ (Cahill *et al.* 2001) also has some chemical (but not structural) features in common with these minerals, but it contains fluorine in addition to $(OH)^–$, and it shows partial replacement of P^{5+} by S^{6+}, with charge balance being maintained *via* the coupled $P^{5+}(OH)^- \rightleftarrows S^{6+}O^{2-}$ substitution.

Several phosphates, as reviewed by Huminicki & Hawthorne (2002), have structures consisting of infinite chains of (PO_4) tetrahedra and $(Al\phi_6)$ octahedra (where ϕ represents an unspecified ligand). Other examples of minerals with chain structural motifs that were not included in the review and bear structural resemblance with sanjuanite are galliskiite (Kampf *et al.* 2010), kapundaite (Mills *et al.* 2010), and the synthetic phases $Pb_3Fe^{3+}_2(PO_4)_4(H_2O)$ (Mills *et al.* 2010), $PbIn(AsO_4)(AsO_3OH)$ (Kolitsch & Schwendtner 2005) and $Na_{2.88}Fe(PO_4)_2$ (Hatert 2007) However, the group formed by *pairs* of double chains of alternating (PO_4) and (AlO_6) present in sanjuanite has no exact counterpart in any known mineral.

ACKNOWLEDGEMENTS

We are grateful to H.D. Gay and R. Lira for providing the sanjuanite sample. A.R. Kampf, the late R. Bideaux, I. Kiseleva and M. Bisengalieva are acknowledged for sending references. L. Reinaudi kindly translated a paper written in Russian. We gratefully acknowledge the suggestions and corrections made by S. Marincea, H. Effenberger, R. Frost, an anonymous reviewer and R.F. Martin. One of the authors (J.R.) thanks the Spanish Ministerio de Ciencia e Innovación Tecnológica (Projects MAT2009–07967, Consolider NANOSELECT CSD2007–00041) and the Generalitat de Catalunya (SGR2009) for financial support. R.E.C. thank FONCYT (project PICT2007 00303), CONICET (PIP 5767) and SECYT–UNC for financial support. E.V. P.-M. thanks CONICET for a fellowship.

REFERENCES

ABELEDO, M.E.J. DE, ANGELELLI, V., BENYACAR, M.A.R. DE & GORDILLO, C.E. (1968): Sanjuanite, a new hydrated basic sulfate–phosphate of aluminum. *Am. Mineral.* **53**, 1-8.

ALLMANN, R. (1975): Beziehungen zwischen Bindungslängen und Bindungsstärken in Oxidstrukturen. *Monatsh. Chem.* **106**, 779-793.

AMOS, A.J. (1954): Observaciones de las formaciones paleozoicas de La Rinconada, pie oriental de la Sierra Chica del Zonda (San Juan). *Rev. de la Asoc. Geol. Argent.* **9**, 5-38.

ANGELELLI, V., BRODTKORB, M.K. DE, GORDILLO, C.E. & GAY, H.D. (1983): *Las Especies Minerales de la República Argentina*. Secretaría de Industria y Minería, Servicio Minero Nacional, Buenos Aires, Argentina.

ASSAOUDI, H. & ENNACIRI, A. (1997): Vibrational spectra and structure of rare earth orthophosphates, weinschenkite type. *Spectrochim. Acta* **A53**, 895-902.

BARAN, E. J., PEDREGOSA, J. C. & AYMONINO, P. J. (1974): The vibrational spectra of strontium and barium diarsenates. *J. Mol. Structure* **22**, 377-387.

BÄRLOCHER, C. (1995): Restraints and constraints in Rietveld refinement. *In* The Rietveld Method (R.A. Young, ed.). Oxford University Press, Oxford, U.K. (186-196).

Beukes, G.J., Schoch, A.E., van der Westhuizen, W.A., Bok, L.D.C. & de Bruiyn, H. (1984): Hotsonite, a new hydrated aluminum-phosphate–sulphate from Pofadder, South Africa. *Am. Mineral.* **69**, 979-983.

Brückner, S. (2000): Estimation of the background in powder diffraction patterns through a robust smoothing procedure. *J. Appl. Crystallogr.* **33**, 977-979.

Cahill, C.L., Krivovichev, S.V., Burns, P.C., Bekenova, G.K. & Shabanova, T.A. (2001): The crystal structure of mitryaevaite $Al_5(PO_4)_2[(P,S)O_3(OH,O)]_2F_2(OH)_2(H_2O)_8$• $6.48H_2O$, determined from a microcrystal using synchrotron radiation. *Can. Mineral.* **39**, 179-186.

Cardinali, A.L. (1985): Génesis del sulfato de aluminio y formación de yacimientos económicamente explotables. *1° Jornadas sobre Geología de Precordillera, Proc.* I, 365-369.

Cardinali, A.L. (1999): Sulfatos de aluminio, magnesio y hierro, San Juan. *In* Recursos Minerales de la República Argentina (E.O. Zappettini, ed.). *Instituto de Geología y Recursos Minerales, SEGEMAR, Anales* **35**, 733-735.

Castro Luna, A.E., Ponzi, M.I., Narda, G.E. & Pedregosa, J.C. (1994): Infrared spectroscopic and X-ray diffraction characterization of Mn/Ni/P catalyst. *J. Mater. Sci. Lett.* **13**, 1749-1750.

Chakhmouradian, A.R., Cooper, M.A., Medici, L., Hawthorne, F.C. & Adar, F. (2008): Fluorine-rich hibschite from silicocarbonatite, Afrikanda Complex, Russia: crystal chemistry and conditions of crystallization. *Can. Mineral.* **46**, 1033-1042.

Cheetham, A.K. (1995) *Ab initio* structure solution with powder diffraction data. *In* The Rietveld Method (R.A. Young, ed.). Oxford University Press, New York, N.Y. (276-292).

de Bruiyn, H., Beukes, G.J., van der Westhuizen, W.A. & Tordiffe, E.A.W. (1989): Unit cell dimensions of the hydrated aluminium phosphates–sulphate minerals sanjuanite, kribergite and hotsonite. *Mineral. Mag.* **53**, 385-386.

du Rietz, T. (1945): Kribergite, ett nyt mineral från Kristinebergs gruva I Västerbottens lan. *Geol. Fören. Stockholm Förh.* **67**, 78-79.

Dykstra, M., Kneller, B. & Milana, J.P. (2006): Deglacial and postglacial sedimentary architecture in a deeply incised paleovalley-paleofjord – the Pennsylvanian (late Carboniferous) Jejenes Formation, San Juan, Argentina. *Geol. Soc. Am., Bull.* **118**, 913-937.

Grey, I.E., Madsen, I.C., Mills, S.J., Hatert, F., Peterson, V.K. & Bastow, T.J. (2010): A new type of cubic-stacked layer structure in anthoinite, $AlWO_3(OH)_3$. *Am. Mineral.* **95**, 639-645.

Hatert, F. (2007): Crystal structure of trisodium iron diphosphate, $Na_{2.88}Fe(PO_4)_2$, a synthetic phosphate with hannayite-type heteropolyhedral chains. *Z. Kristallogr.* **222**, 6-8.

Huminicki, D.M.C. & Hawthorne, F.C. (2002): The crystal chemistry of the phosphate minerals. *In* Phosphates – Geochemical, Geobiological, and Materials Importance (M.J. Kohn, J. Rakovan & J.M. Hughes, eds.). *Rev. Mineral. Geochem.* **48**, 123-253.

Ivanov, O.K. Shiryaeva L.L., Khoroshilova L.A. & Petrisheva V.G. (1990): Hotsonite: confirmation of the discovery and new data (Belyavinsky mine, the Urals). *Zap. Vser. Mineral. Obshchest.* **119**, 121-126 (in Russian).

Kampf, A.R., Colombo, F., Simmons, W.B., Falster, A.U. & Nizamoff, J.W. (2010): Galliskiite, $Ca_4Al_2(PO_4)_2F_8$•$5H_2O$, a new mineral from the Gigante granitic pegmatite, Córdoba province, Argentina. *Am. Mineral.* **95**, 392-396.

Kolitsch, U. & Schwendtner, K. (2005): Octahedral–tetrahedral framework structures of $InAsO_4$•H_2O and $PbIn(AsO_4)(AsO_3OH)$. *Acta Crystallogr.* **C61**, i86-i89.

Kneller, B., Milana, J.P., Buckee, C. & al Ja'aidi, O. (2004): A depositional record of deglaciation in a paleofjord (Late Carboniferous [Pennsylvanian] of San Juan Province, Argentina): the role of catastrophic sedimentation. *Geol. Soc. Am., Bull.* **116**, 348-367.

Langford, J.I. & Louër, D. (1996): Powder diffraction. *Rep. Prog. Phys.* **59**, 131-234.

Lazebnik, K.A., Zakayina, N.V. & Supletsov, V.M. (1998): The first find of the rare mineral sanjuanite in Russia. *Dokl. Akad. Nauk, Earth Science Sect.* **362**, 233-235 (in Russian).

Le Bail, A., Stephens, P.W. & Hubert, F. (2003): A crystal structure of the souzalite/gormanite series from synchrotron powder diffraction data. *Eur. J. Mineral.* **15**, 719-723.

Libowitzky, E. (1999): Correlation of O–H stretching frequencies and O–H….O hydrogen bond lengths in minerals. *Monatsh. Chem.* **130**, 1047-1059.

Márquez Zavalía, M.F. & Pedregosa, J.C. (1994): Cyanotrichite and carbonato-cyanotrichite in Capillitas mine, Catamarca. *Rev. Asoc. Geol. Argent.* **49**, 353-358.

Mills, S.J., Birch, W.D., Kampf, A.R., Christy, A.G., Pluth, J.J., Pring, A., Raudsepp, M. & Chen, Yu-Sheng (2010): Kapundaite, $(Na,Ca)_2Fe^{3+}{}_4(PO_4)_4(OH)_3$•$5H_2O$, a new phosphate species from Tom's quarry, South Australia: description and structural relationship to mélonjosephite. *Am. Mineral.* **95**, 754-760.

Mills, S.J., Kolitsch, U., Miyawaki, R., Hatert, F., Poirier, G., Kampf, A.R., Matsubara, S. & Tillmanns, E. (2010): $Pb_3Fe^{3+}{}_2(PO_4)_4(H_2O)$, a new octahedral–tetrahedral framework structure with double-strand chains. *Eur. J. Mineral.* **22**, 595-604.

Moraes, P.A., Romano, R., Souza Filho, A.G., Freire, P.T.C., Mendes Filho, J. & Alves, O.L. (2006): Vibrational spectra of α-$Ge(HPO_4)_2$•H_2O compound. *Vib. Spectrosc.* **40**, 209-212.

Müller, A. & Krebs, B. (1967): Normal coordinate treatment of XY_4-type molecules and ions with T_d symmetry. I. Force constants of a modified valence force field and of the Urey–Bradley force field. *J. Mol. Spectrosc.* **24**, 180-197.

Myneni, S.C.B. (2000): X-ray and vibrational spectroscopy of sulfate in earth materials. *In* Sulfate Minerals – Crystallography, Geochemistry and Environmental Significance (C.N. Alpers, J.L. Jambor & D.K. Nordstrom, eds.). *Rev. Mineral. Geochem.* **40**, 113-172.

Perchiazzi, N., Ondruš, P. & Skála, R. (2004): Ab initio X-ray powder structure determination of parascorodite, $Fe(H_2O)_2AsO_4$. *Eur. J. Mineral.* **16**, 1003-1007.

Pujana, R. (2005): Gymnospermous woods from Jejenes Formation, Carboniferous of San Juan, Argentina: *Abietopitys petriellae* (Brea and Césari) nov. comb. *Ameghiniana* **42**, 725-731.

Rietveld, H.M. (1969): A profile refinement method for nuclear and magnetic structures. *J. Appl. Crystallogr.* **2**, 65-71.

Rius, J. (1993): Derivation of a new tangent formula from Patterson function arguments. *Acta Crystallogr.* **A49**, 406-409.

Rius, J. (2009a): RIBOLS18: a computer program for restrained Rietveld refinement. Institut de Ciència de Materials de Barcelona (CSIC), Barcelona, Spain.

Rius, J. (2009b): DAJUST1: a computer program for extracting integrated intensities from powder data. Institut de Ciència de Materials de Barcelona (CSIC), Barcelona, Spain.

Rius, J. (2011): Patterson-function direct methods for structure determination of organic compounds from powder data. XVI. *Acta Crystallogr.* **A67**, 63-67.

Rius, J., Elkaim, E. & Torrelles, X. (2004): Structure determination of the blue mineral pigment aerinite from synchrotron powder diffraction data: the solution of an old riddle. *Eur. J. Mineral.* **16**, 127-134.

Rius, J., Louër, D., Louër, M., Galí, S. & Melgarejo, J.C. (2000): Structure solution from powder data of the phosphate hydrate tinticite. *Eur. J. Mineral.* **12**, 581-588.

Rius, J., Miravitlles, C., Amigó, J.M., Reventós, M.M. & Louër, D. (1996): Determination of crystal structures from powder diffraction data by direct methods: extraction of integrated intensities from partially overlapping intensities *Anales de Química Int. Ed.* **92**, 223-227.

Rius, J. & Plana, F. (1982): Una nueva función que relaciona la longitud de enlace iónico con la valencia electrostática del catión. *Anales de Química* **80 B**, 147-149.

Schoch, A.E., Beukes, G.J. & Praekelt, H.E. (1985): A natroalunite – zaherite – hotsonite paragenesis from Pofadder, Bushmanland, South Africa. *Can. Mineral.* **23**, 29-34.

Wallwork, K.S., Pring, A., Taylor, M.R. & Hunter, B.A. (2002): The structure of priceite, a basic hydrated calcium borate, by *ab initio* powder-diffraction methods. *Can. Mineral.* **40**, 1199-1206.

Wallwork, K.S., Pring, A., Taylor, M.R. & Hunter, B.A. (2003): A model for the structure of the hydrated aluminum phosphate, kingite determined by *ab initio* powder diffraction methods. *Am. Mineral.* **88**, 235-239.

Werner, P.-E. (1984): TREOR90 software. Deep Structural Chemistry, Arrhenius Lab., University of Stockholm, Stockholm, Sweden.

Received May 8, 2010, revised manuscript accepted May 15, 2011.